

NEUTRINO CONSTRAINTS TO SCOTOGENIC DARK MATTER INTERACTING IN THE SUN

T. de Boer[†], R. Busse^{‡,*}, A. Kappes[‡], M. Klasen[†], S. Zeinstra[†]

[†]*Institut für Theoretische Physik/* [‡]*Institut für Kernphysik, Westfälische Wilhelms-Universität Münster, Wilhelm-Klemm-Str. 9, 48149 Münster, Germany*



Radiative seesaw models have the attractive property of providing dark matter candidates in addition to generation of neutrino masses. Here we present a study of neutrino signals from the annihilation of dark matter particles which have been gravitationally captured in the Sun, in the framework of the scotogenic model. We compute expected event rates in the ICECUBE detector in its 86-string configuration. As fermionic dark matter does not accumulate in the Sun, we study the case of scalar dark matter, with a scan over the parameter space. Due to a naturally small mass splitting between the two neutral scalar components, inelastic scattering processes with nucleons can occur. We find that for small mass splittings, the model yields very high event rates. If a detailed analysis at ICECUBE can exclude these parameter points, our findings can be translated into a lower limit on one of the scalar couplings in the model. For larger mass splittings only the elastic case needs to be considered. We find that in this scenario the XENON1T limits exclude all points with sufficiently large event rates.

1 Introduction

While there is strong evidence for the existence of large amounts of dark matter in the universe, the nature of dark matter is still unknown. Radiative seesaw models, like the famous scotogenic model¹, present an interesting solution to this problem, while at the same time only extending the Standard Model (SM) by very few fields.

In the framework of the scotogenic model, WIMPs (weakly interacting massive particles) can accumulate in large celestial bodies like the Sun. The WIMPs can lose energy by scattering off nuclei inside the Sun, until they are gravitationally captured and sink into the core, producing a local over-density which results in a boost of self-annihilation. The WIMPs can either annihilate directly into neutrinos or into other SM particles, which in turn decay into neutrinos. This produces a flux that can be measured by neutrino telescopes such as ICECUBE².

The accumulation of dark matter in the Sun is directly linked to the WIMP-nucleon scattering cross section. In this work, we consider both elastic and inelastic scattering. The latter arises through a natural mass splitting of the two neutral components in the case of scalar dark matter in the scotogenic model. We investigate the parameter space by means of a numerical

scan, in order to identify models that yield sufficiently large neutrino event rates in ICECUBE in its IC86 string configuration, and could therefore be studied in future ICECUBE analyses.

2 The scotogenic model

The scotogenic model extends the Standard Model by two new fields: One fermion singlet N_i with three generations, and one scalar doublet with the components (η^+, η^0) . An additional \mathbb{Z}_2 symmetry, under which the new fields are odd and all Standard Model fields are even, ensures the stability of the lightest odd particle by preventing its further decay. The lightest odd particle is the dark matter candidate of the scotogenic model, provided it is neutral¹.

The new terms to the Lagrangian are:

$$\mathcal{L}_N = -\frac{m_{N_i}}{2} N_i N_i + y_{i\alpha} \left(\eta^\dagger L_\alpha \right) N_i + \text{h.c.} - V, \quad (1)$$

$$\begin{aligned} V = & m_\phi^2 \phi^\dagger \phi + m_\eta^2 \eta^\dagger \eta + \frac{\lambda_1}{2} \left(\phi^\dagger \phi \right)^2 + \frac{\lambda_2}{2} \left(\eta^\dagger \eta \right)^2 + \lambda_3 \left(\phi^\dagger \phi \right) \left(\eta^\dagger \eta \right) \\ & + \lambda_4 \left(\phi^\dagger \eta \right) \left(\eta^\dagger \phi \right) + \frac{\lambda_5}{2} \left[\left(\phi^\dagger \eta \right)^2 + \left(\eta^\dagger \phi \right)^2 \right] \end{aligned} \quad (2)$$

where m_{N_i} is the mass matrix of the fermion singlet, the L_α are the left-handed Standard Model lepton doublets with $\alpha = 1, 2, 3$ generations, $y_{i\alpha}$ is a Yukawa coupling matrix where $i = 1, 2, 3$ are the generations of the new right-handed neutrinos, the λ_{1-5} are the new coupling parameters, and ϕ is the Standard Model Higgs field.

After electroweak symmetry breaking, the squared masses of the new physical scalar bosons are given by

$$\begin{aligned} m_{\eta^+}^2 &= m_\eta^2 + \lambda_3 \langle \phi^0 \rangle^2, \\ m_{\eta^{0R}}^2 &= m_\eta^2 + (\lambda_3 + \lambda_4 + \lambda_5) \langle \phi^0 \rangle^2, \\ m_{\eta^{0I}}^2 &= m_\eta^2 + (\lambda_3 + \lambda_4 - \lambda_5) \langle \phi^0 \rangle^2, \end{aligned} \quad (3)$$

where $\langle \phi^0 \rangle = 246.22/\sqrt{2} \text{ GeV}$ is the Higgs vacuum expectation value³. The real and imaginary components of the neutral scalar η^0 , indicated by the superscripts R and I , respectively, obtain slightly different masses. This mass splitting δ is governed by the coupling parameter λ_5 , which must be naturally small, since if λ_5 is exactly zero, the neutrinos would be massless and lepton number would be conserved, leading to a larger symmetry. For bounds on the other model parameters, please refer to Ref.⁴.

3 WIMP-nucleon scattering in the Sun

In contrast to fermion dark matter, scalar dark matter has a non-zero spin-independent WIMP-nucleon cross section which enables accumulation in the Sun. The diagrams for scalar dark matter scattering off of nucleons are shown in Fig. 1 (left hand side). Next to elastic scattering, the existence of a slightly heavier state allows for inelastic scattering as well, where the dark matter particle transitions into the heavier state, provided that the mass splitting δ between the two states fulfills $\delta < \frac{v^2}{2} \mu$, where μ is the WIMP nucleon reduced mass and v is the relative velocity⁵. For small λ_5 the mass splitting can be approximated by:

$$\delta \approx \frac{\lambda_5 \langle \phi^0 \rangle^2}{m_{\eta^{0R/I}}}, \quad (4)$$

depending on the smaller of the masses $m_{\eta^{0R}}$ and $m_{\eta^{0I}}$. This shows the dependence of the mass splitting on λ_5 explicitly.⁴

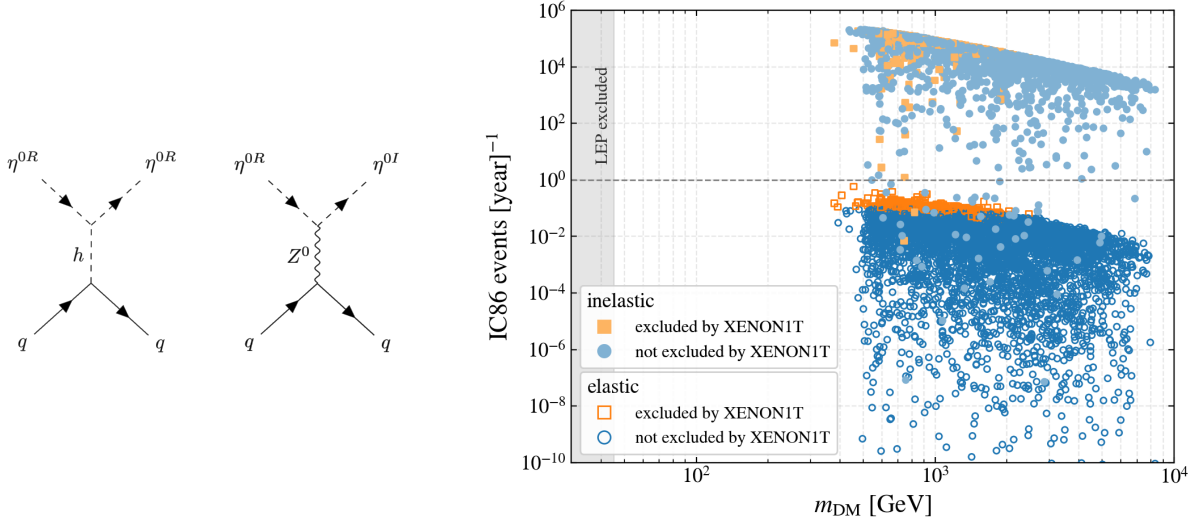


Figure 1 – **Left:** Feynman diagrams of the elastic and inelastic scalar dark matter-nucleon scattering processes in the scotogenic model. In this case the dark matter candidate is η^{0R} . For the case where η^{0I} is the dark matter candidate, one can replace η^{0R} with η^{0I} and vice versa. **Right:** Event rate in IC86 vs. the mass of the dark matter candidate. Models with a small mass splitting between η^{0R} and η^{0I} , for which inelastic scattering dominates, are marked with filled points. Models with larger mass splittings are marked with hollow points. For both cases, orange points are excluded by XENON1T, while blue points are not. The grey dashed line marks one IC86 event per year. The grey shaded area marks masses that are excluded by the LEP limit from the invisible Z^0 width.

The inelastic scattering off of quarks in the scotogenic model is mediated by a Z^0 -exchange. The amplitude can be decomposed into a vector and an axial-vector part. For scalar dark matter, the axial-vector part vanishes in the non relativistic limit⁶. The remaining vector interaction contributes to the spin-independent scattering cross section.

4 Results of the numerical scan

To investigate the scotogenic model numerically, we implement the model using SARAH 4.14.0⁷. The mass spectrum and branching ratios are then computed with SPHENO 4.0.3^{8,9}, and observables such as the relic density and neutrino fluxes are calculated using MICROMEGAS 5.0.8¹⁰. Since the inelastic scenario was not implemented in MICROMEGAS, we use CALCHEP 3.7¹¹ to calculate the the WIMP-quark matrix elements and the cross section in the inelastic case. The inelastic capture rate is calculated with DARKSUSY-6.2.3¹² and inserted into modified MICROMEGAS routines. For the elastic scenario we use pre-existing MICROMEGAS routines for both the scattering cross section as well as the capture rate. The event rate in IC86 is calculated with a modified routine in MICROMEGAS, with the latest data for the ICECUBE effective area¹³.

Figure 1 (right hand side) shows results of our numerical scan. The IC86 event rate is plotted against the mass of the dark matter particle. We see two groups of models: The lower group consists mainly of models with a large mass splitting between η^{0R} and η^{0I} , for which inelastic scattering is kinematically forbidden. The upper group with significantly higher event rates consists of models with small mass splittings and dominant inelastic dark matter. Note that we show only those points that survive the following constraints: PLANCK relic density¹⁴, the mass of the Higgs boson¹⁵, LFV limits^{16,17,18}, and limits on the Standard Model neutrino masses (we use the Casas-Ibarra parametrization¹⁹ to calculate the Yukawa coupling matrix). We plot also the LEP exclusion from the invisible Z^0 width^{20,21}, to show that it does not constrain our parameter space. The remaining models can further be constrained by direct detection limits, where the XENON1T limit on the spin-independent WIMP-nucleon cross section²² imposes the

strongest and only constraint to our parameter space. In both groups of models we draw the XENON-excluded ones in orange, whereas in the inelastic group they are excluded for their elastic scattering cross section, since the XENON limit does not apply to inelastic dark matter.

We see that no model in the elastic group yields ICECUBE event rates above one event per year, whereas almost all models in the inelastic group do, up to event rates of $\mathcal{O}(10^5)$ per year. The non-excluded inelastic models could therefore be probed by ICECUBE. The findings of a respective analysis can be translated into a lower limit of the coupling parameter λ_5 .

5 Summary

In this work we investigated neutrino signals from WIMP annihilations in the Sun within the framework of the scotogenic model. We performed a numerical scan of the parameter space, in order to identify models that yield an IC86 event rate above one event per year, and are viable under a number of experimental constraints. Both elastic and inelastic dark matter have been considered. We find that elastic dark matter yields IC86 event rates of only $\mathcal{O}(10^{-1})$, while for inelastic dark matter there exist viable models with event rates up to $\mathcal{O}(10^5)$. The findings of an ICECUBE analysis probing these models could be translated into a lower limit on the coupling parameter λ_5 of the scotogenic model.

Acknowledgments

This work has been supported by the BMBF and the DFG through the Research Training Group 2149 "Strong and weak interactions – from hadrons to dark matter".

References

1. E. Ma, *Phys. Rev. D* 73 (2006) 077301, Preprint hep-ph/0601225.
2. M. G. Aartsen, et al., *JINST* 12 (03) (2017) P03012, Preprint 1612.05093.
3. P. A. Zyla, et al., *PTEP* 2020 (8) (2020) 083C01.
4. T. de Boer, R. Busse, A. Kappes, M. Klasen, S. Zeinstra, Preprint 2105.04899.
5. D. Tucker-Smith, N. Weiner, *Phys. Rev. D* 64 (2001) 043502, Preprint hep-ph/0101138.
6. P. Agrawal, Z. Chacko, C. Kilic, R. K. Mishra, Preprint 1003.1912.
7. F. Staub, *Comput. Phys. Commun.* 185 (2014) 1773–1790, Preprint 1309.7223.
8. W. Porod, *Comput. Phys. Commun.* 153 (2003) 275–315, Preprint hep-ph/0301101.
9. W. Porod, F. Staub, *Comput. Phys. Commun.* 183 (2012) 2458–2469, Preprint 1104.1573.
10. G. Bélanger, F. Boudjema, A. Goudelis, A. Pukhov, B. Zaldivar, *Comput. Phys. Commun.* 231 (2018) 173–186, Preprint 1801.03509.
11. A. Belyaev, N. D. Christensen, A. Pukhov, *Comput. Phys. Commun.* 184 (2013) 1729–1769, Preprint 1207.6082.
12. T. Bringmann, J. Edsjö, P. Gondolo, P. Ullio, L. Bergström, *JCAP* 07 (2018) 033, Preprint 1802.03399.
13. M. Aartsen, et al., *Eur. Phys. J. C* 77 (3) (2017) 146, Preprint 1612.05949, [Erratum: *Eur.Phys.J.C* 79, 214 (2019)].
14. N. Aghanim, et al., *Astron. Astrophys.* 641 (2020) A6, Preprint 1807.06209.
15. G. Aad, et al., *Phys. Rev. Lett.* 114 (2015) 191803, Preprint 1503.07589.
16. A. M. Baldini, et al., *Eur. Phys. J. C* 76 (8) (2016) 434, Preprint 1605.05081.
17. U. Bellgardt, et al., *Nucl. Phys. B* 299 (1988) 1–6.
18. C. Dohmen, et al., *Phys. Lett. B* 317 (1993) 631–636.
19. J. Casas, A. Ibarra, *Nucl. Phys. B* 618 (2001) 171–204, Preprint hep-ph/0103065.
20. Q.-H. Cao, E. Ma, G. Rajasekaran, *Phys. Rev. D* 76 (2007) 095011, Preprint 0708.2939.
21. E. Lundstrom, M. Gustafsson, J. Edsjo, *Phys. Rev. D* 79 (2009) 035013, Preprint 0810.3924.
22. E. Aprile, et al., *Phys. Rev. Lett.* 121 (11) (2018) 111302, Preprint 1805.12562.